

Theoretical Analysis of Two-Phase Bubble Formation in an Immiscible Liquid

W. B. Chen and Reginald B. H. Tan

Dept. of Chemical and Environmental Engineering, National University of Singapore,
Singapore 119260, Singapore

Two-phase bubble formation coupled with phase change at a submerged nozzle is studied theoretically. The whole bubble consists of a vapor and a liquid phase. The inner vapor phase is assumed to be surrounded by a thin condensate layer, in which the vapor condenses partially as the two-phase bubble grows. The interface element approach is applied to describe the dynamics of bubble formation. The effect of heat transfer from bulk vapor within the bubble to the surrounding bulk liquid is related to pressure analysis of vapor within the two-phase bubble via the mass flux of condensation. The results computed from this model agree well with the experimental data.

Introduction

The dispersion of gases through submerged orifices or nozzles plays an important role in enhancing the transport rates between phases in many chemical and physical processes. In many industrial heat exchange operations, a condensable gas is often injected into a liquid through a submerged orifice or nozzle to increase the rate of heat transfer between the gas and liquid, as direct contact heat transfer has the advantage of high heat transfer coefficient. Denekamp et al. (1972), Cho and Lee (1990), and Chen and Tan (2001) have studied vapor bubble formation at submerged nozzle in its own liquid, that is, the processes studied involve only one component. When the dispersed and continuous phases are formed by two different immiscible components instead of one component, a two-phase particle can be observed during bubble formation. It contains a liquid and a vapor phase, the vapor accumulating in the inner part of the particle. Being neither a pure drop nor a pure vapor phase, this two-phase bubble has been referred to as a drobble (Sudhoff et al., 1982). The latter system differs from the former, one-component, system in that the condensate remains within the confines of the bubble envelope.

Owing to their wide application in industrial heat-transfer processes, two-phase bubbles have been extensively studied both experimentally and theoretically. Sideman and Hirsch (1965) photographed condensing isopentane bubbles in water during their free rise period, or after their release from the nozzle. By analyzing consecutive pictures of each run, the instantaneous surface area, volume and vapor content of a ris-

ing drobble could be determined and the heat flux and transfer coefficients obtained. Jacobs et al. (1978) proposed a model for the collapse of a bubble rising through a cold continuous immiscible liquid. Wanchoo (1991) investigated the condensation of a rising two-phase bubble in immiscible liquid and derived an analytic expression for the steady rate of heat transfer from a two-phase bubble condensing in an immiscible liquid medium. Wanchoo et al. (1997) measured experimentally the velocity of rise and the drag of a single vapor bubble collapsing in another immiscible liquid. Sudhoff et al. (1982) reviewed the published studies since 1963 on the condensation or evaporation of a drobble and summarized the overall heat-transfer coefficients measured for various systems. More recently, Kalman and Ullmann (1999) conducted a series of experiments of direct-contact condensation to the initial volume of a condensing bubble released from an orifice and the instantaneous shapes of drobble during the collapse process. Their experimental results showed that the initial volume of the condensing bubble could be reasonably predicted by employing Ruff's two-stage model (Ruff, 1972) that was originally developed for noncondensing bubbles.

Most of the above studies deal with the collapse of condensing drobble after its release from the nozzle. However, it is known that the period of bubble formation can contribute significantly to the overall heat and mass transfer of the process. Few reported investigations have been published on the formation of two-phase bubbles. Terasaka et al. (1999) proposed a method to measure the heat-transfer coefficient for direct-contact condensation during two-phase bubble formation and theoretically estimated the direct-contact heat-transfer coefficient. Terasaka et al. (2000) proposed a drobble for-

Correspondence concerning this article should be addressed to R. B. H. Tan.

mation model to study the effect of operating conditions on two-phase bubble formation behavior at single nozzle submerged in water. The equations of motion for expansion and translation of an equivalent spherical bubble were used.

The objective of this article is to study the hydrodynamics of two-phase bubble formation combined with the mechanism of heat transfer, and to gain theoretical understanding of two-phase bubble formation with condensation at a single submerged nozzle. A realistic nonspherical model for bubble formation coupled with phase change is described. The model attempts to calculate the instantaneous shape of the drobble during its formation and to determine the instantaneous volumes of both whole bubble and condensate, frequency of bubble formation, as well as overall heat-transfer coefficient. The effects of gas flow rate and temperature difference between injected gas and the subcooled liquid will be discussed.

A bubble formation model, which can predict bubble shapes, bubble growth, and detachment under different thermal and hydrodynamic conditions, would significantly add to our understanding of some dispersion processes, which involve condensable gas and liquid direct contact. The present model should provide useful predictions of the characteristics of a phase-change bubble in the single-bubbling region and provide the basis for design and optimization of such processes.

Model Development

Physical system and basic equations

The system under consideration consists of a condensable gas that is injected vertically upwards through a single nozzle R_o submerged in a liquid (bulk temperature T_l) of depth h at a constant flow rate Q . The following basic assumptions are made:

(a) The bubble remains symmetrical about its axis during the growth and is a volume of revolution around its central axis.

(b) The influence of gas and liquid viscosities at the interface is negligible.

(c) The growth of the bubble is unaffected by the presence of other bubbles.

(d) The gas is ideal, isothermal, and incompressible and its flow is adiabatic.

(e) The dispersed phase is a pure substance. There are no noncondensable gases in the dispersed phase.

(f) Vapor condensate and continuous liquid are immiscible or the dissolution of vapor condensate into continuous liquid is negligible.

(g) Energy exchange across vapor-condensate interface is dominated by mass transfer due to condensation and the energy exchange by heat transfer is neglected.

(h) The gravitational effect on the thickness of the condensate layer is negligible and the thickness of the condensate layer is assumed to be uniform, as it is much smaller than the radius of the drobble.

Figure 1 shows the nonspherical model for two-phase bubble formation at a submerged nozzle. The nonspherical bubble formation model proposed by Tan and Harris (1986) is modified to calculate the movement of the interface elements. This approach assumes the instantaneous bubble shape is axially symmetric and divides the interface between

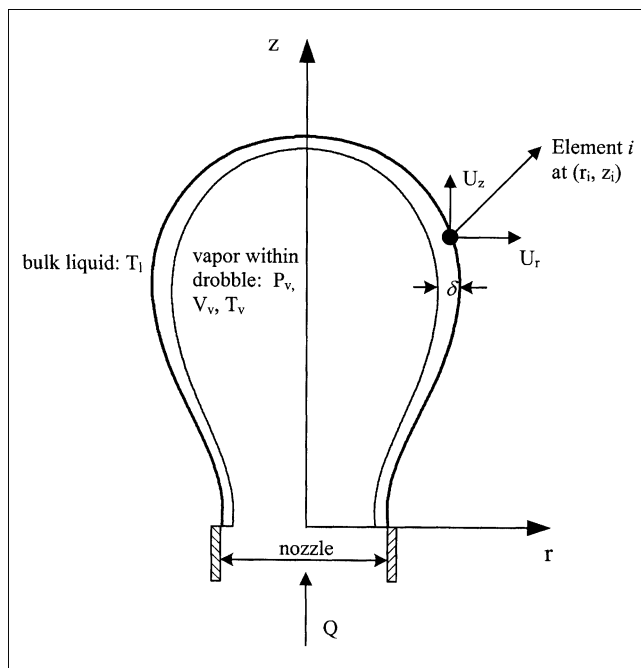


Figure 1. Nonspherical bubble formation with phase change.

the two-phase bubble and the bulk liquid into a finite number of small elements. Assuming an inviscid liquid, each element at the bubble interface moves as a result of forces due to pressure difference and surface tension. In dynamic formation, the resultant of these forces is equal to the rate of change in the liquid momentum, assuming that the gas momentum is negligible. The momentum of the liquid may be calculated using the “added mass” concept and the velocity of the interface. Thus, a force balance at each element generates a set of differential equations of motion in cylindrical coordinates

$$r\Delta P dr - \sigma(r \sin \beta) = \frac{d}{dt}(U_z \bar{m})_i \quad (1)$$

$$r\Delta P dz + \sigma \left[d(r \cos \beta) - \frac{dz}{\sin \beta} \right] = \frac{d}{dt}(U_r \bar{m})_i \quad (2)$$

where r and z are the radial coordinate from the axis of the bubble and the axial coordinate from the orifice horizontal level, respectively, ΔP is the pressure difference between bubble pressure P_v and the liquid pressure P_l at each interface element. β is an angle defined by

$$\beta = \tan^{-1} \frac{\partial z}{\partial r} \quad (3)$$

The second term in the lefthand side of Eqs. 1 and 2 is the force due to surface tension. There are two kinds of surface tensions (surface tension between vapor and condensate, and interfacial tension between condensate and liquid) acting on a two-phase bubble, as a two-phase bubble consists of double interfaces. The condensate thickness is very small when compared with the bubble equivalent radius, and the surface ten-

sion defined in Eqs. 1 and 2 is expressed as

$$\sigma = \sigma_{vc} + \sigma_{cl} \quad (4)$$

where σ_{vc} and σ_{cl} are surface tensions between vapor and condensate, and surface tension between condensate and liquid, respectively.

The term \bar{m}_i in Eqs. 1 and 2 is the differential added mass

$$\bar{m}_i = (\alpha \rho_l + \rho_b) V_i \quad (5)$$

where α is the added mass coefficient, taken as 0.5, the value for a bubble translating in an infinite medium (Walters and Davidson, 1963). This is regarded to be an average value during the whole formation process. V_i is the volume of liquid displaced by the element since the beginning of its movement. ρ_l and ρ_b are the density of the bulk liquid and the two-phase bubble, respectively. The mean density of the two-phase bubble is estimated by

$$\rho_b = \frac{\rho_v V_v + \rho_c V_c}{V_b} \quad (6)$$

where ρ_v , ρ_c , V_v , V_c , and V_b are vapor density, condensate density, vapor volume, condensate volume and whole bubble volume, respectively.

The vapor volume is obtained from the application for the mass balance

$$V_v = \frac{Q \rho_v t - V_c \rho_c}{\rho_v} \quad (7)$$

where Q is the constant flow rate of gas injected into the bubble, t is the bubble growth time.

Taking the vapor within the two-phase bubble as a non-steady state open system, from the application for the mass balance and the first law of thermodynamics for a nonsteady-state open system, the derivation of pressure change of the vapor within the two-phase bubble can be expressed as

$$\frac{dP_v}{dt} = \frac{\gamma R_g T_v}{V_v} \left(\frac{P_v Q}{R_g T_v} - \frac{j A_c}{M} \right) - \frac{\gamma P_v}{V_v} \frac{dV_v}{dt} + (\gamma - 1) \frac{\rho_v Q^3}{2 V_v a_o^2} \quad (8)$$

where γ , R_g , T_v , j , A_c , M , and a_o are the adiabatic gas constant, gas constant, vapor temperature, mass flux of condensation, surface area of condensate, molecular weight of dispersed phase, and cross-sectional area of the nozzle, respectively.

The liquid pressure P_l at each interfacial element is computed by

$$P_l = P_s + \rho_l g(h - z) \quad (9)$$

where P_s is the system pressure above the bulk liquid.

Effect of heat transfer and condensation

During the drobble formation, the dispersed vapor partially condenses to form a condensate layer when the boiling point of vapor is higher than the temperature of the bulk

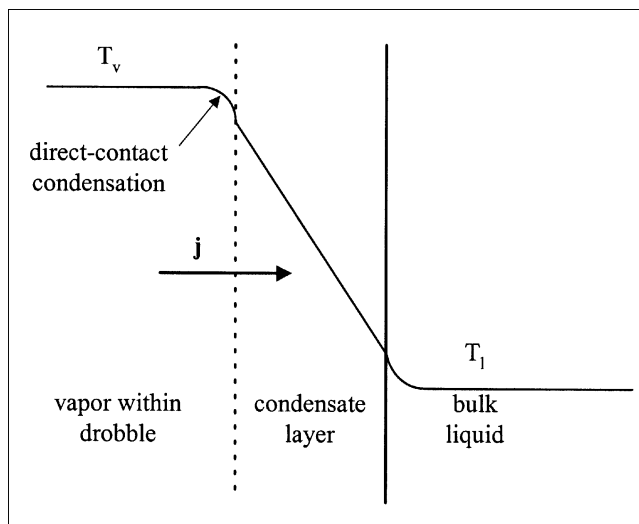


Figure 2. Physical model for heat transfer from bulk vapor within drobble into surrounding bulk liquid through a thin condensate layer.

liquid. Figure 2 illustrates the mechanism of heat transfer with condensation during the two-phase bubble growth. The vapor within the drobble is rapidly mixed so that the temperature of the bulk vapor is assumed to be constant at its boiling point T_v .

The overall heat-transfer coefficient U for heat transfer from the bulk vapor within the drobble into the surrounding bulk liquid through a thin condensate layer is calculated generally as

$$\frac{1}{U} = \frac{1}{H_g} + \frac{1}{H_d} + \frac{1}{H_c} + \frac{1}{H_l} \quad (10)$$

where H_g , H_d , H_c , and H_l are the heat-transfer coefficients for convection in vapor phase, direct-contact condensation, conduction in the condensate layer, and convection in bulk liquid, respectively.

Compared with H_d and H_c , heat-transfer coefficients for convection in vapor and liquid phases are much higher and their contribution to U can be neglected. Thus, the overall heat-transfer coefficient is estimated as

$$\frac{1}{U} = \frac{1}{H_d} + \frac{1}{H_c} \quad (11)$$

The calculation of direct contact heat-transfer coefficient H_d was proposed by Terasaka et al. (1999) to be

$$H_d = L \sqrt{\frac{2 \rho_v}{T_v (T_v - T_l) (1/\rho_v - 1/\rho_c)}} \quad (12)$$

where L is the latent heat of vaporization.

Also, the heat-transfer coefficient H_c is given by

$$H_c = \frac{k_c}{\delta} \quad (13)$$

where k_c and δ are the thermal conductivity and the thickness of the condensate, respectively.

The thickness of the condensate layer is much smaller than the radius of the drobble. Assuming uniform thickness, the thickness of the condensate layer δ is approximated as

$$\delta = \frac{V_c}{A_c} \quad (14)$$

Both the thickness of the condensate layer and the mass flux are taken as functions of time only. They are related by the heat flux continuity condition

$$jL = \Delta T \times U = \frac{T_v - T_l}{\frac{1}{H_d} + \frac{\delta}{k_c}} \quad (15)$$

The instantaneous condensation mass rate m_c is defined by

$$m_c = jA_c \quad (16)$$

The total accumulated condensate volume V_c at bubble growth time t can be obtained

$$V_c = \frac{1}{\rho_c} \int_0^t m_c dt \quad (17)$$

Rewriting Eq. 17 in differential form

$$\frac{dV_c}{dt} = \frac{jA_c}{\rho_c} \quad (18)$$

Initial conditions and numerical solution

At the beginning of the computation, the bubble shape is assumed to be hemispherical, with its radius equal to that of

the nozzle. Initially, both thickness and volume of the condensate film are zero.

The dynamic equations for drobble formation can be solved with the following initial conditions

$$r = R_o, V_c = 0, \delta = 0, P_v = P_s + \rho_l gh + \frac{2\sigma}{R_o} \quad j = \frac{\Delta TH_d}{L} \quad (19)$$

An explicit finite difference method proposed by Tan and Harris (1986) is extended to solve the equations of bubble formation. The computational procedure is summarized in the following steps:

- (1) Initialize all parameters.
- (2) Increase bubble growth time by Δt .
- (3) Solve the equations of motion for each element to yield new coordinates of each element.
- (4) Compute the bubble volume and heat-transfer area by numerical integration of coordinates of all elements.
- (5) Apply straightforward Runge-Kutta method to solve the differential Eqs. 8 and 18 simultaneously to obtain the instantaneous vapor pressure P_v and condensate volume V_c .
- (6) Compute the instantaneous vapor volume V_v , condensate thickness δ , and condensation mass flux j by solving Eqs. 7, 14 and 15, respectively.
- (7) Compute the pressure difference for each element at the bubble interface.
- (8) Return to step 2 and repeat steps 2–6 until the neck closes and detachment is attained.

Results and Discussion

The two-phase bubble formation model is applied to hexane/water system and vinyl acetate/water system. The surface tension of hexane/water $\sigma = \sigma_{vc} + \sigma_{cl} = 0.0504 + 0.0138$

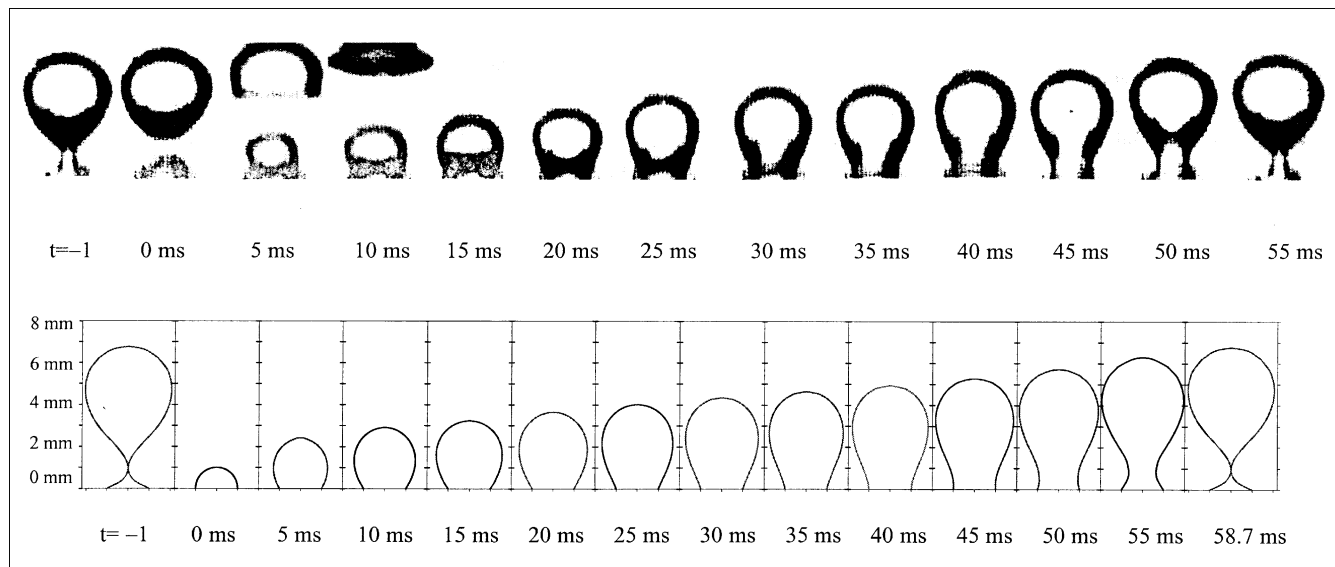


Figure 3. Two-phase bubble growth sequences for experimental conditions: system = hexane/water, $Q = 3.38 \times 10^{-6} \text{ m}^3/\text{s}$, $R_o = 1.00 \times 10^{-3} \text{ m}$, $\Delta T = 7.0 \text{ K}$.

(a) Experimental photograph from Terasaka et al. (1999); (b) computed bubble shapes by present model.

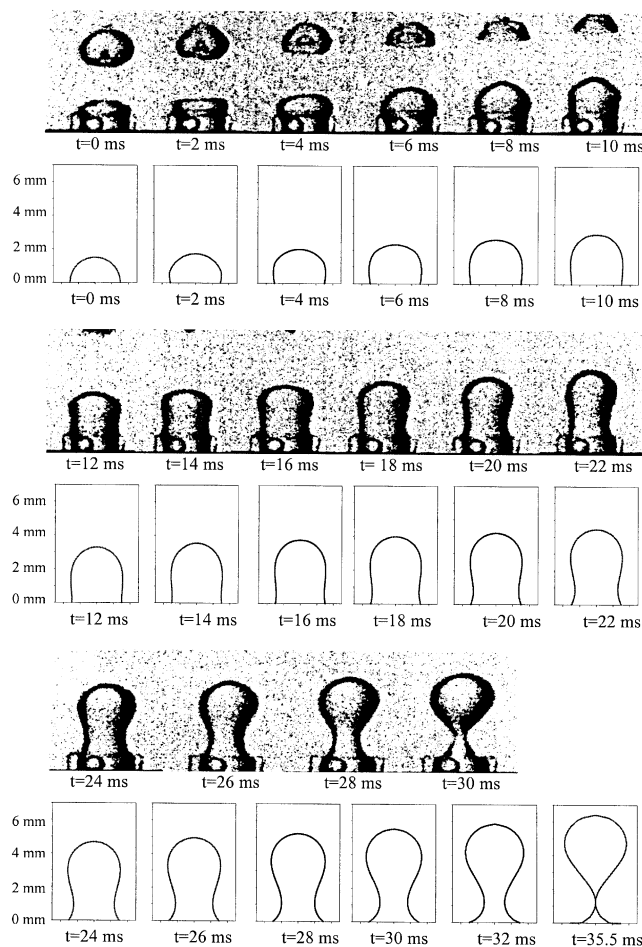


Figure 4. Two-phase bubble growth sequences for experimental conditions: system = vinyl acetate/water, $Q = 5.8 \times 10^{-6} \text{ m}^3/\text{s}$, $R_o = 1.50 \times 10^{-3} \text{ m}$, $\Delta T = 18.9 \text{ K}$.

$= 0.0642 \text{ N/m}$. For vinyl acetate/water system, $\sigma = \sigma_{vc} + \sigma_{cl} = 0.0187 + 0.00713 = 0.02583 \text{ N/m}$ (Prakoso et al., 2001).

Two-phase bubble shapes during formation

Figure 3 shows the two-phase bubble growth sequences for the case of a hexane/water system, $Q = 3.38 \times 10^{-6} \text{ m}^3/\text{s}$, $R_o = 1.00 \times 10^{-3} \text{ m}$, $\Delta T = 7.0 \text{ K}$, corresponding to the experimental conditions in Terasaka et al. (1999). The bubble growth time interval between two consecutive contours is $5 \times 10^{-3} \text{ s}$, and the final shape shows neck closure and, hence, detachment. Both the experimental and computed bubble shapes indicate that bubble shapes during formation are non-spherical. A bubble starts off as a hemisphere with its radius the same as that of the nozzle, then becomes approximately spherical as it grows, and finally attains the shape of an irregular ellipsoid with a neck. The computed instantaneous bubble shapes are in very good agreement with the experimental video images taken by Terasaka et al. (1999).

Figure 4 shows another example of two-phase bubble formation; the conditions are: vinyl acetate/water $Q = 5.8 \times 10^{-6} \text{ m}^3/\text{s}$, $R_o = 1.50 \times 10^{-3} \text{ m}$, $\Delta T = 18.9 \text{ K}$, which are the experimental conditions in Prakoso et al. (2001). This figure shows

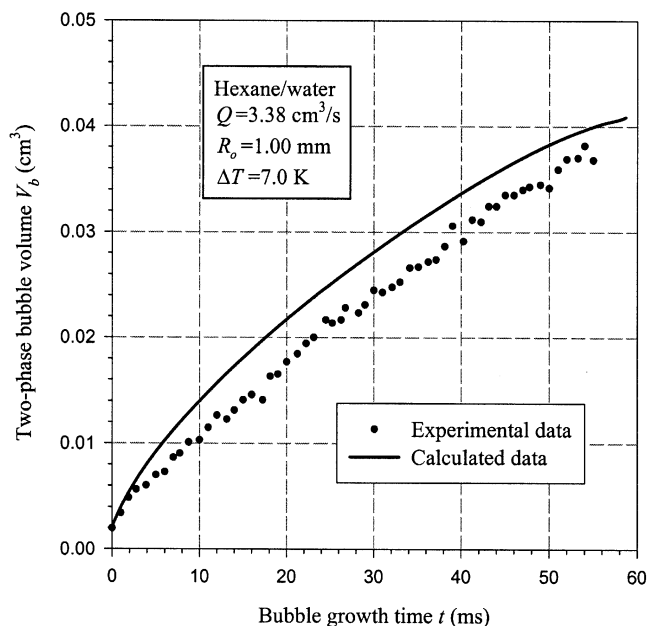


Figure 5. Two-phase bubble growth rates for bubble formation at conditions: system = hexane/water, $Q = 3.38 \times 10^{-6} \text{ m}^3/\text{s}$, $R_o = 1.00 \times 10^{-3} \text{ m}$, $\Delta T = 7.0 \text{ K}$.

a similar trend of bubble shapes during formation as that in Figure 3. The system studied in Figure 4 differs from that in Figure 3 in that the condensate of vinyl acetate is slightly soluble in water. The effect of this dissolution rate on bubble formation has been neglected in our modeling. The predicted shapes correlate well with the experimental video images taken by Prakoso et al. (2001) except that the experimental detachment time is a little shorter than predicted by our model. This is probably due to the effect of condensate dissolution, which would hasten detachment by accelerating the thinning of the bubble neck in the final stages.

Two-phase bubble growth rates

The comparison of the bubble growth rates between the results computed by the present model with the experimental data at conditions corresponding to Figure 3 are plotted in Figure 5. The volumes of the growing bubbles in Figure 5 were measured by Terasaka et al. (1999) using high-speed video camera (1,000 frames per second), with data capture and image analysis. The figure indicates that the predicted rate of growth by the present model follows closely the experimental data (Terasaka et al., 1999).

Figure 6 shows the variation of bubble growth rates with temperature difference ΔT for the conditions hexane/water, $Q = 4.0 \times 10^{-6} \text{ m}^3/\text{s}$, $R_o = 0.50 \times 10^{-3} \text{ m}$, corresponding to the experimental run in Prakoso et al. (2001). Simulated results are compared with the experimental data available (Prakoso et al., 2001) for the effects of temperature difference ΔT on the two-phase bubble growth rates. It indicates the two-phase bubble grows faster and detaches earlier for the case of lower temperature difference. It can be seen that our model predicts the experimental trends reasonably well.

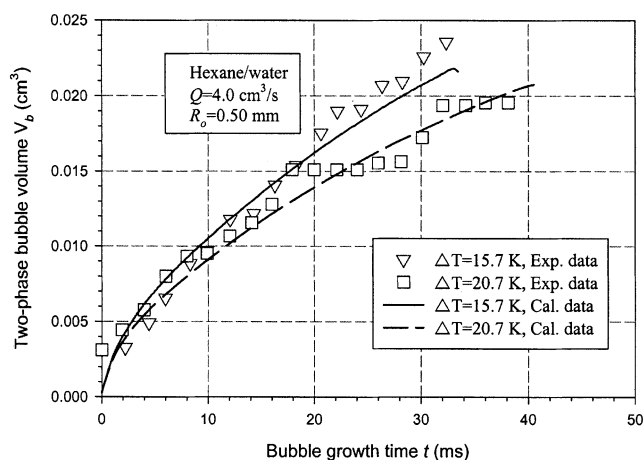


Figure 6. Effect of temperature difference ΔT on two-phase bubble growth rates.

Figure 7 shows the effect of gas-flow rate Q at constant temperature difference ΔT on bubble growth rates for the conditions hexane/water, $R_o = 0.50 \times 10^{-3}$ m, $\Delta T = 15.7$ K, corresponding to the experimental run in Prakoso et al. (2001). The two-phase bubble volume is smaller when the injected gas-flow rate is lower as expected empirically. This trend was also observed experimentally for one component bubble formation without condensation. From the experimental curve of $Q_o = 3.2$ cm³/s, it appears that delayed release occurs, during which a bubble remains attached to the nozzle without growing significantly (McCann and Prince, 1971). It can be noted again that the model predictions match the experimental data rather well.

Volume and thickness of condensate layer

Figure 8 shows the computed volume and thickness of condensate layer during bubble formation at conditions corresponding to Figure 3. It can be seen that the volume of condensate is smaller by several orders of magnitude than that of the whole two-phase bubble. The thickness of condensate

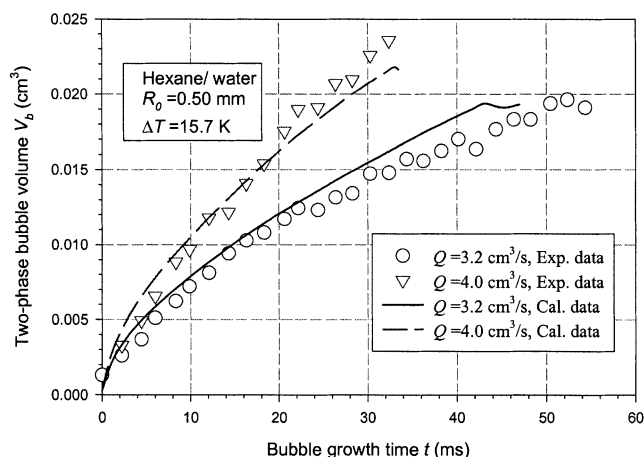


Figure 7. Effect of gas-flow rate on two-phase bubble growth rates.

layer is also smaller by several orders of magnitude than the average radius of the whole bubble at the same bubble growth time. Therefore, the assumption made in Eq. 14 is reasonable.

It is worth remarking that video images such as those in Figures 3 and 4 cannot provide an accurate indication of the condensate layer thickness, since the bubble curvature and light refraction would distort the true liquid film thickness.

Overall heat-transfer coefficient and condensation ratio

Figure 9 shows the instantaneous overall heat-transfer coefficient U for bubble formation at conditions corresponding to Figure 3. The instantaneous overall experimental heat-transfer coefficients were obtained from experimental observations by a heat and mass balance (Terasaka et al., 1999) as follows

$$U = \frac{L}{A_c \Delta T} \left(Q - \frac{dV_v}{dt} \right) \quad (20)$$

Overall heat-transfer coefficient decreases rapidly at the beginning of bubble growth. The direct contact heat-transfer coefficient H_d is equal to the overall heat-transfer coefficient U at the very beginning of bubble growth, when the condensate film has not been generated.

To determine whether inertial and buoyancy effects on the one hand, or heat-transfer effect on the other hand, is more dominant in the two-phase bubble formation process, it is necessary to estimate the vapor condensation ratio. The vapor condensation ratio is defined as the ratio of condensate mass to the mass of the whole two-phase bubble at detachment. The former can be calculated from the condensate density and volume. The latter is equal to the mass of vapor injected through the nozzle during each bubble formation period. A high vapor condensation ratio indicates a dominance of heat transfer over inertial and buoyancy effects, and vice versa.

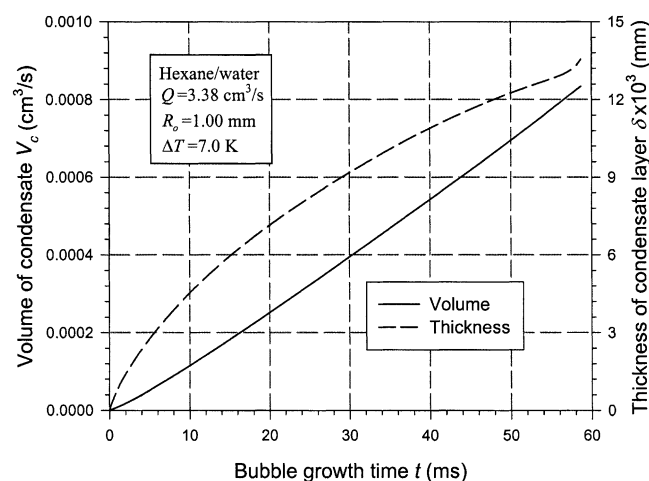


Figure 8. Volume and thickness of condensate layer during bubble formation at conditions: system = hexane/water, $Q = 3.38 \times 10^{-6}$ m³/s, $R_o = 1.00 \times 10^{-3}$ m, $\Delta T = 7.0$ K.

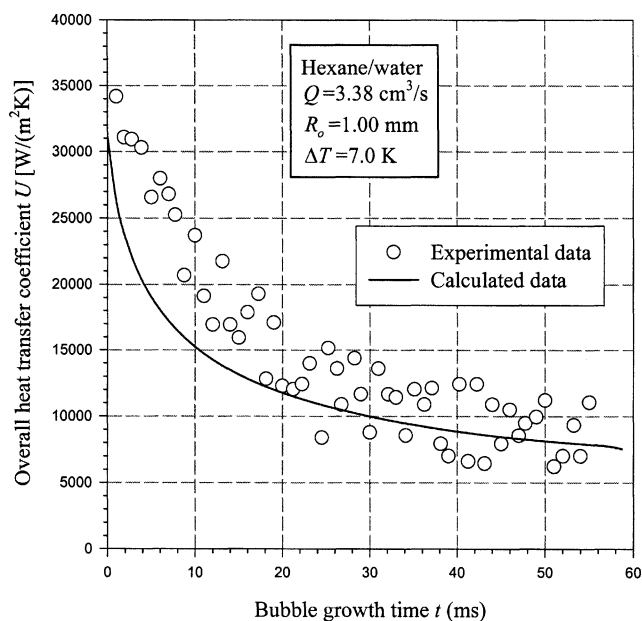


Figure 9. Instantaneous overall heat-transfer coefficient at conditions: system=hexane/water, $Q=3.38 \times 10^{-6} \text{ m}^3/\text{s}$, $R_0=1.00 \times 10^{-3} \text{ m}$, $\Delta T=7.0 \text{ K}$.

Figure 10 shows the effect of temperature difference between vapor and bulk liquid on the vapor condensate ratio at bubble detachment, for several values of gas-flow rates. It shows a significant proportion of vapor condensation (50–90%) occurs during the formation process. It also shows an increase in vapor condensation ratio with increase of temperature difference and decrease of gas-flow rate, indicating an increase in dominance of heat-transfer effect over inertial and buoyancy effects.

Conclusion

Two-phase bubble formation at a submerged nozzle in an immiscible liquid is analyzed theoretically. The interfacial el-

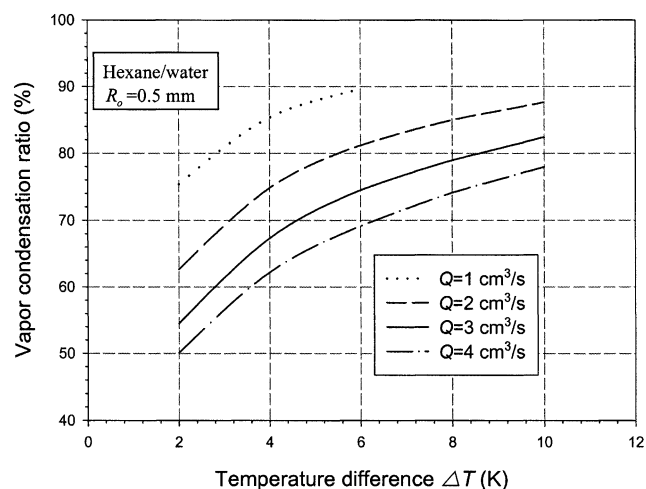


Figure 10. Effect of temperature difference on vapor condensation ratio.

ement approach successfully models the physical phenomena of both hydrodynamics and heat transfer during a two-phase bubble formation. The method generates realistic bubble shapes during formation and subsequent detachment. The simulated results in terms of instantaneous bubble shape, bubble volume, bubble growth rate as well as overall heat transfer are in good agreement with the experimental data from Terasaka et al. (1999) and Prakoso et al. (2001)

Notation

- a_o = cross-sectional area of the nozzle, m^2
- A_c = surface area of condensate, m^2
- C_p = constant-pressure heat capacity, $\text{J}/(\text{mol} \cdot \text{K})$
- C_v = constant-volume heat capacity, $\text{J}/(\text{mol} \cdot \text{K})$
- e_v = molar internal energy of vapor within two-phase bubble, J/mol
- E_v = internal energy of vapor within two-phase bubble, J
- $E_{k,in}$ = kinetic energy of gas injected into bubble, J
- g = acceleration due to gravity, m/s^2
- h = height of liquid above the nozzle trip, m
- h_c = molar enthalpy of condensate, J/mol
- h_{in} = molar enthalpy of gas injected into bubble, J/mol
- H_c = heat-transfer coefficient for conduction in condensate layer, $\text{W}/(\text{m}^2 \cdot \text{K})$
- H_d = direct contact heat-transfer coefficient, $\text{W}/(\text{m}^2 \cdot \text{K})$
- H_g = heat-transfer coefficient for convection in bulk vapor phase, $\text{W}/(\text{m}^2 \cdot \text{K})$
- H_l = heat-transfer coefficient for convection in bulk liquid phase, $\text{W}/(\text{m}^2 \cdot \text{K})$
- j = condensation mass flux, $\text{kg}/(\text{m}^2 \cdot \text{s})$
- k_c = thermal conductivity of condensate, $\text{W}/(\text{m} \cdot \text{K})$
- L = latent heat of vaporization, J/kg
- m_c = condensation mass rate, kg/s
- \bar{m}_i = differential added mass of the element, kg
- M = molecular weight of dispersed phase, kg/mol
- n = molar number of vapor within two-phase bubble, mol
- n_d = molar number of condensate, mol
- n_{in} = molar number of gas injected into bubble, mol
- P_l = liquid pressure on bubble surface, Pa
- P_s = system pressure above bulk liquid, Pa
- P_v = vapor pressure of two-phase bubble, Pa
- ΔP = pressure difference between bubble pressure and liquid pressure at interface, Pa
- Q = gas constant flow rate, m^3/s
- r = radial coordinate from axis of bubble, m
- R_g = gas constant, $\text{J}/(\text{mol} \cdot \text{K})$
- R_o = nozzle radius, m
- t = bubble growth time, s
- T_l = bulk liquid temperature, K
- T_v = temperature of vapor within the two-phase bubble, K
- U = overall heat-transfer coefficient, $\text{W}/(\text{m}^2 \cdot \text{K})$
- U_x = horizontal velocity of element, m/s
- U_z = vertical velocity of element, m/s
- V_b = whole volume of two-phase bubble, m^3
- V_c = condensate volume, m^3
- V_i = volume of liquid displaced by the element since the beginning of its movement, m^3
- V_v = volume of vapor within the two-phase bubble, m^3
- W = work interaction across vapor-condensate interface, J
- z = axial coordinate from orifice horizontal level, m

Greek letters

- α = added mass coefficient, dimensionless
- β = angle defined by Eq. 3, dimensionless
- γ = adiabatic gas constant, dimensionless
- δ = condensate thickness, m
- Θ = heat interaction across vapor-condensate interface, J
- ρ_b = mean density of two-phase bubble, kg/m^3
- ρ_c = condensate density, kg/m^3
- ρ_l = bulk liquid density, kg/m^3
- ρ_v = density of vapor within the two-phase bubble, kg/m^3

σ = surface tension, N/m
 σ_{vc} = surface tension between vapor and condensate, N/m
 σ_{cl} = surface tension between condensate and liquid, N/m

Literature Cited

- Chen, W. B., and R. B. H. Tan, "A Model for Steam Bubble Formation at a Submerged Nozzle in Flowing Subcooled Water," *Int. J. Heat and Fluid Flow*, **22**, 552 (2001).
 Cho, S. C., and W. K. Lee, "A Model for Steam Bubble Formation at a Submerged Orifice in a Flowing Liquid," *J. Chem. Eng. Jpn.*, **23**, 180 (1990).
 Denekamp, J., A. Kogan, and A. Solan, "On the Condensation of an Injected Vapor Bubble in a Subcooled Liquid Stream," *Prog. Heat Mass Transfer*, **6**, 179 (1972).
 Jacobs, H. R., H. Fannar, and G. C. Beggs, "Collapse of a Bubble of Vapor in an Immiscible Liquid," *Proc. Sixth Int. Heat Transfer Conf.*, Toronto, 383 (1978).
 Kalman, H., and A. Ullmann, "Experimental Analysis of Bubble Shapes During Condensation in Miscible and Immiscible Liquids," *J. Fluid Eng.*, **121**, 496 (1999).
 McCann, D. J., and R. G. H. Prince, "Regimes of Bubbling at a Submerged Orifice," *Chem. Eng. Sci.*, **26**, 1505 (1971).
 Prakoso, T., K. Terasaka, and H. Tsuge, "Effect of Operating Conditions on Two-Phase Bubble Formation Behavior at Single Nozzle Submerged in Water," *J. Chem. Eng. Jpn.*, **34**, 114 (2001).
 Ruff, K., "Formation of Gas Bubbles at Nozzles with Constant Throughput," *Chem. Ing. Techn.*, **44**, 1360 (1972).
 Sideman, S., and G. Hirsch, "Direct Contact Heat Transfer with Change of Phase," *AIChE J.*, **11**, 1019 (1965).
 Sudhoff, B., M. Plischke, and P.-M. Weinspach, "Direct Contact Heat Transfer with Change of Phase-Condensation or Evaporation of a Drobble," *Ger. Chem. Eng.*, **5**, 24 (1982).
 Tan, R. B. H., and I. J. Harris, "A Model for Non Spherical Bubble Growth at a Single Orifice," *Chem. Eng. Sci.*, **41**, 3175 (1986).
 Terasaka, K., W.-Y. Sun, T. Prakoso, and H. Tsuge, "Measurement of Heat Transfer Coefficient for Direct-Contact Condensation during Bubble Growth in Liquid," *J. Chem. Eng. Jpn.*, **32**, 594 (1999).
 Terasaka, K., T. Prakoso, W.-Y. Sun, and H. Tsuge, "Two-Phase Bubble Formation with Condensation at Nozzle Submerged in Immiscible Liquid," *J. Chem. Eng. Jpn.*, **33**, 113 (2000).
 Walters, J. K., and J. F. Davidson, "Initial Motion of Gas Bubble Formed in Inviscid Liquid," *J. Fluid Mech.*, **17**, 321 (1963).
 Wanchoo, R. K., "Condensation of Single Two-Phase Bubbles in an Immiscible Liquid: Heat Transfer Characteristics," *Chem. Eng. Comm.*, **105**, 99 (1991).
 Wanchoo, R. K., S. K. Sharma, and G. K. Raina, "Drag Coefficient and Velocity of Rise of a Single Collapsing Two-Phase Bubble," *AIChE J.*, **43**, 1955 (1997).

Appendix: Derivation of Vapor Pressure Change

The total mass balance for the vapor within the two-phase bubble is

$$dn = dn_{in} - dn_c \quad (A1)$$

where n_{in} and n_c are the molar number of gas injected into bubble and condensate, respectively, and

$$\frac{dn_{in}}{dt} = \frac{P_v Q}{R_g T_v} \quad (A2)$$

$$\frac{dn_c}{dt} = \frac{d}{dt} \left(\frac{V_c \rho_c}{M} \right) = \frac{\rho_c}{M} \frac{dV_c}{dt} = \frac{\rho_c}{M} \times \frac{jA_c}{\rho_c} = \frac{jA_c}{M} \quad (A3)$$

where P_v and T_v are the pressure and temperature of the vapor, respectively. V_c , A_c , and ρ_c are volume, surface area, and density of the condensate.

Applying open system energy balance (or first law of thermodynamics for open system) to the vapor within the two-phase bubble, the internal energy change of vapor within the two-phase bubble dE_v can be expressed in terms of heat interaction across the vapor-condensate interface $d\Theta$, work interaction across the vapor-condensate interface dW , and energy balance due to nonsteady flow (the last three terms in the righthand side of Eq. A4)

$$dE_v = d\Theta + dW + h_{in} dn_{in} - h_c dn_c + dE_{k,in} \quad (A4)$$

Here,

$$dE_v = nde_v + e_v dn \quad (A5)$$

$d\Theta$ is the sensible enthalpy increase, which, in general, is negligible compared with latent heat effects from mass transfer and condensation, so

$$d\Theta = 0 \quad (A6)$$

$$dW = -P_v dV_v \quad (A7)$$

$$dE_{k,in} + \frac{\rho_v}{2} \left(\frac{Q}{a_o} \right)^2 Q dt \quad (A8)$$

Substituting the above expressions into Eq. A4, it follows that

$$nC_v dT_v + P_v dV_v = R_g T_v dn + \frac{\rho_v}{2} \left(\frac{Q}{a_o} \right)^2 Q dt \quad (A9)$$

Rewriting Eq. A9 together with ideal gas law equation

$$P_v V_v = nR_g T_v \quad (A10)$$

After substituting Eqs. A2 and A3, the pressure change of vapor within the two-phase bubble is obtained

$$\frac{dP_v}{dt} = \frac{\gamma R_g T_v}{V_v} \left(\frac{P_v Q}{R_g T_v} - \frac{jA_c}{M} \right) - \frac{\gamma P_v}{V_v} \frac{dV_v}{dt} + (\gamma - 1) \frac{\rho_v Q^3}{2V_v a_o^2} \quad (Eq. 8)$$

where γ is the adiabatic gas exponent

$$\gamma = \frac{C_p}{C_v} \quad (A11)$$

and C_p and C_v are constant-pressure and constant-volume heat capacities, respectively.

Manuscript received July 3, 2001, and revision received Feb. 4, 2003.